

PAPER • OPEN ACCESS

Investigation of a temperature tolerant InGaP (GaInP) converter layer for a ^{63}Ni betavoltaic cell

To cite this article: S Butera *et al* 2017 *J. Phys. D: Appl. Phys.* **50** 345101

View the [article online](#) for updates and enhancements.

Related content

- [Al_{0.52}In_{0.48}P_{0.55}Fe x-ray-photovoltaic battery](#)
S Butera, G Lioliou, A B Krysa et al.
- [Demonstration of a High Open-Circuit Voltage GaN Betavoltaic Microbattery](#)
Cheng Zai-Jun, San Hai-Sheng, Chen Xu-Yuan et al.
- [Design optimization of GaAs betavoltaic batteries](#)
Haiyanag Chen, Lan Jiang and Xuyuan Chen

Investigation of a temperature tolerant InGaP (GaInP) converter layer for a ^{63}Ni betavoltaic cell

S Butera¹, M D C Whitaker¹, A B Krysa² and A M Barnett¹

¹ Semiconductor Materials and Devices Laboratory, School of Engineering and Informatics, University of Sussex, Brighton, BN1 9QT, United Kingdom

² EPSRC National Centre for III–V Technologies, University of Sheffield, Mappin Street, Sheffield, S1 3JD, United Kingdom

E-mail: S.Butera@sussex.ac.uk

Received 8 May 2017, revised 19 June 2017

Accepted for publication 26 June 2017

Published 2 August 2017



Abstract

A prototype InGaP p^+i-n^+ mesa photodiode was studied for its potential as the energy conversion device in a ^{63}Ni betavoltaic cell; its electrical performance was analysed across the temperature range $-20\text{ }^\circ\text{C}$ to $100\text{ }^\circ\text{C}$. The results show that the InGaP detector when illuminated with a laboratory ^{63}Ni radioisotope beta particle source had a maximum output power of $0.92\text{ }^\mu\text{W}$ at $-20\text{ }^\circ\text{C}$, this value decreased at higher temperatures. A decrease in the open circuit voltage and in the cell internal conversion efficiency were also observed when the temperature was increased: at $-20\text{ }^\circ\text{C}$, the open circuit voltage and the cell internal conversion efficiency had values of 0.69 V and 4% , respectively. A short circuit current of $4.5\text{ }^\mu\text{A}$ was measured at $-20\text{ }^\circ\text{C}$.

Keywords: InGaP, betavoltaic, semiconductors

(Some figures may appear in colour only in the online journal)

1. Introduction

Betavoltaic microbatteries are promising systems for the provision of long-term energy (>10 years) supplies for low power consuming technologies such as implantable medical devices [1], FPGA encryption keys [2], and various security and defence technologies. In direct conversion radioisotope microbatteries, since the emissions of the radioisotope are incident on the semiconductor converter layer for the life time of the battery [3], radiation tolerant semiconductor materials are needed. Wide bandgap semiconductor detectors are particularly attractive for betavoltaic microbatteries; in addition to radiation hardness, they can also offer higher conversion efficiencies than narrower bandgap materials, where the conversion efficiency increases linearly with bandgap [4].

Furthermore, due to their low thermally generated leakage currents, wide bandgap materials can work at high temperatures without cooling systems, thus providing compact technologies that can be used in hot environments (e.g. hot deserts and industrial applications) as well as cold environments (e.g. Arctic and Antarctic research stations). Betavoltaic microbatteries that use wide bandgap materials as converter devices have been developed and characterised at room temperature [5–7] and across temperature ranges [8–14]. Si and GaAs structures were successfully used in ^{63}Ni and ^{147}Pm betavoltaic microbatteries by Wang *et al* [13] in the temperature range $-60\text{ }^\circ\text{C}$ to $60\text{ }^\circ\text{C}$; a GaAs ^{147}Pm betavoltaic cell was also demonstrated by Tang *et al* [14] between $-50\text{ }^\circ\text{C}$ and $50\text{ }^\circ\text{C}$. A ^{63}Ni 4H-SiC betavoltaic cell was studied by Chandrashekhar *et al* [12] at temperatures from $24\text{ }^\circ\text{C}$ to $86\text{ }^\circ\text{C}$. III–V phosphide semiconductors have also recently received research attention as promising converter materials in betavoltaic microbatteries; the performances of an $\text{Al}_{0.52}\text{In}_{0.48}\text{P}$ ^{63}Ni betavoltaic cell were reported by Butera *et al* [8] in the temperature range $-20\text{ }^\circ\text{C}$ to

 Original content from this work may be used under the terms of the [Creative Commons Attribution 3.0 licence](https://creativecommons.org/licenses/by/3.0/). Any further distribution of this work must maintain attribution to the author(s) and the title of the work, journal citation and DOI.

140 °C, whilst Tritium betavoltaic InGaP cells were characterised by Cabauy *et al* [15, 16] at room temperature. AlInP has been also successfully used in x-ray photovoltaic microbattery [17]; whilst an InGaP alphavoltaic device has been reported by Cress *et al* [18]. However, it should be noted that the use of an alpha particle source, with respect to beta or x-ray sources, increases the converter device damage risk, since higher energetic particles impinge on the device. The use of InGaP (direct bandgap of ~1.9 eV for In_{0.5}Ga_{0.5}P at room temperature [19–21]) as converter devices in betavoltaic microbatteries is attractive: firstly, In_{0.5}Ga_{0.5}P has higher linear attenuation coefficients than AlInP and other with bandgap materials, this results in a higher quantum efficiency per unit thickness compared to those of wide bandgap materials such as GaAs, SiC and AlInP; secondly, In_{0.5}Ga_{0.5}P can be grown with high crystalline quality nearly lattice matched with GaAs, thus making commercial production relatively simple; thirdly, because of the relatively large bandgap of In_{0.5}Ga_{0.5}P, it should enable large cell conversion efficiencies and operation at elevated temperatures without cooling (due to low thermally generated leakage currents); fourthly, it should be tolerant to high doses of radiation [18].

This paper describes the electrical performances of an ⁶³Ni In_{0.5}Ga_{0.5}P betavoltaic cell over the temperature range –20 °C and 100 °C. The results show the dependence on temperature of the open circuit voltage, the short circuit current, the maximum output power, and the cell internal conversion efficiency. The ⁶³Ni In_{0.5}Ga_{0.5}P betavoltaic cell, due to the high In_{0.5}Ga_{0.5}P attenuation coefficients, produced higher output power with respect to that produced by the previously published AlInP betavoltaic cell [8], at each temperature studied; it has to be noted that the In_{0.5}Ga_{0.5}P converter detector reported has also a thicker i-layer with respect to the previously used AlInP converter photodiode. The exceptional results obtained are also a consequence of the high performances of the In_{0.5}Ga_{0.5}P detector produced; the crystalline quality of the studied In_{0.5}Ga_{0.5}P structure is very high in comparison to other commonly studied wide bandgap material structures (e.g. GaN) due to the advanced growth and fabrication technique used.

2. Materials and methods

A p⁺–i–n⁺ (5 μm i-layer) In_{0.5}Ga_{0.5}P layer structure was grown on a n⁺ GaAs substrate, using metalorganic vapour phase epitaxy. In order to suppress CuPt type ordering and associated decrease of the bandgap energy of In_{0.5}Ga_{0.5}P [22–24], the substrate's epitaxial surface had a miscut angle of 10° towards ⟨1 1 1⟩A. The details of the In_{0.5}Ga_{0.5}P structure and the metallisation layers are summarised in table 1. Chemical wet etching techniques were used to fabricate a 400 μm diameter In_{0.5}Ga_{0.5}P mesa photodiode: 1:1:1 K₂Cr₂O₇:HBr:CH₃COOH solution was used as the etchant, followed by a 10 s finishing etch in a 1:8:80 H₂SO₄:H₂O₂:H₂O solution. The top Ohmic contact had an annular shape with bondpad, the top metallisation covered 33% of the In_{0.5}Ga_{0.5}P device's top face.

Table 1. Layer details of the In_{0.5}Ga_{0.5}P diode.

Layer	Material	Thickness (μm)	Dopant	Dopant type	Doping density (cm ⁻³)
1	Ti	0.02			
2	Au	0.2			
3	GaAs	0.01	Zn	p ⁺	1 × 10 ¹⁹
4	In _{0.5} Ga _{0.5} P	0.2	Zn	p ⁺	2 × 10 ¹⁸
5	In _{0.5} Ga _{0.5} P	5		undoped	
6	In _{0.5} Ga _{0.5} P	0.1	Si	n ⁺	2 × 10 ¹⁸
7	Substrate				
	n ⁺ GaAs				
8	Au	0.2			
9	InGe	0.02			

The In_{0.5}Ga_{0.5}P mesa diode was illuminated by a standard laboratory 185 MBq ⁶³Ni radioisotope beta source, which was positioned as close as experimentally possible (3 mm) to the top of the In_{0.5}Ga_{0.5}P device in order to maximize the energy deposited by the electrons in the converter device. It has to be noted that 185 MBq was the actual activity of the source; in a best case scenario (i.e. specific activity of 56 mCi mg⁻¹) such a source would have an apparent activity of 172 MBq taking into account self-absorption effects [25]. The ⁶³Ni radioisotope beta source was a Ni foil (7 mm by 7 mm) with ⁶³Ni on one side; to comply with local radiation rules the source had a 1 μm layer of inactive Ni electroplated over the active ⁶³Ni, such that it could be handled as a sealed source. Both the In_{0.5}Ga_{0.5}P detector and the ⁶³Ni radioactive source were placed inside a temperature test chamber (TAS Micro MT); dry nitrogen was constantly flowing inside the chamber to prevent any humidity related effects influencing the measurements (environment relative humidity <5%).

The Monte Carlo computer modeling package CASINO (version 3.3) [26, 27] was used to study the beta particle quantum efficiency of the In_{0.5}Ga_{0.5}P device in the energy range of interest (1 keV to 66 keV). 4000 beta particles were used in each simulation, the beta particles were injected at the p⁺-side of the In_{0.5}Ga_{0.5}P structure. At each electron energy, two slightly different structures were simulated: firstly, we simulated the In_{0.5}Ga_{0.5}P structure without a top metal contact; secondly, we simulated the In_{0.5}Ga_{0.5}P structure with a top metal contact covering all the device surface. A total of 132 simulations were run. Each simulation gave information of where the beta electrons are absorbed in the In_{0.5}Ga_{0.5}P structure; the percentage (QE) of the electron energy absorbed through the 5 μm i-layer In_{0.5}Ga_{0.5}P device with respect to the electron energy incident on the face of the cell was quantified. Quantum efficiency values for the structure without a top metal contact (QE_{NC}) and for the structure with a top metal contact (QE_C) were obtained. Since the top metal contact only covered 33% of the device surface, the percentage (QE_i) of the energy deposited by beta electrons of various energy in the In_{0.5}Ga_{0.5}P i-layer was calculated from a weighted sum of QE_{NCi} and QE_{Ci}; the calculated QE_i are shown in figure 1.

Following the simulations of the beta particle quantum efficiency of the device, modelling was conducted to simulate the

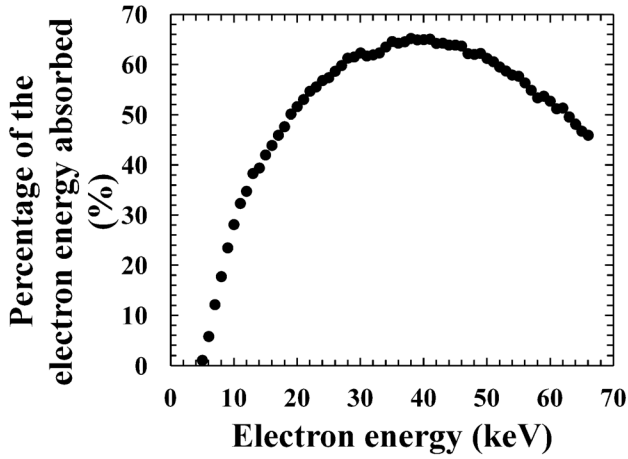


Figure 1. Beta particle quantum efficiency (percentage of electron energy absorbed) in the $\text{In}_{0.5}\text{Ga}_{0.5}\text{P}$ i-layer as a function of the beta electron energy, as determined by Monte Carlo modelling.

attenuation of the beta electrons through the protective inactive Ni over-layer ($1 \mu\text{m}$ thick) of the specific radioisotope beta particle source use in the experimental characterizations. It was found that the beta electrons with energies $<20 \text{ keV}$ were primarily attenuated by the inactive Ni over-layer. If a real-world betavoltaic battery were to be made, the inactive Ni over-layer would not be present, but for the purposes of the semiconductor device characterisation reported here the over-layer was necessary to comply with laboratory safety protocols. Attenuation of the beta particles in the dry nitrogen gap (3 mm) was determined to be negligible compared to the other losses.

The expected electrical power (P_{th}) extracted from the $\text{In}_{0.5}\text{Ga}_{0.5}\text{P}$ betavoltaic cell was calculated according to equation (1):

$$P_{\text{th}} = \sum_{i=0}^{\text{endpoint}=66} \frac{A}{2} \frac{Em_i}{A_{\text{Ni}}} \frac{A_{\text{InGaP}}}{A_{\text{Ni}}} \text{QE}'_i \frac{i}{\omega_{\text{InGaP}}} 1.6 \times 10^{-19} \quad (1)$$

where A was the apparent activity of the ^{63}Ni source (172 MBq, under the approximation of an highly pure ^{63}Ni radioactive source), Em_i was the emission probability of an electron of energy i after taking into account self-absorption effects, A_{Ni} was the area of the ^{63}Ni source, A_{InGaP} was the area of the $\text{In}_{0.5}\text{Ga}_{0.5}\text{P}$ detector, QE'_i was the percentage of each electron energy absorbed in the $\text{In}_{0.5}\text{Ga}_{0.5}\text{P}$ i-layer considering also attenuation through the protective inactive Ni over-layer, ω_{InGaP} the $\text{In}_{0.5}\text{Ga}_{0.5}\text{P}$ electron-hole pair creation energy (4.8 eV, 2.5 times the bandgap). Due to the source-detector system geometry, only half of the beta electrons were emitted towards the $\text{In}_{0.5}\text{Ga}_{0.5}\text{P}$ device; thus, the apparent activity of the ^{63}Ni radioactive source was halved for use in equation (1). P_{th} was found to be 26 pW. It should be noted that a best case scenario (highly pure ^{63}Ni) was assumed here in order to produce the most conservative (pessimistic) betavoltaic efficiencies in section 3.

3. Results and discussion

A Keithley 6487 picoammeter/voltage source was used to measure the current across the $\text{In}_{0.5}\text{Ga}_{0.5}\text{P}$ diode as function of

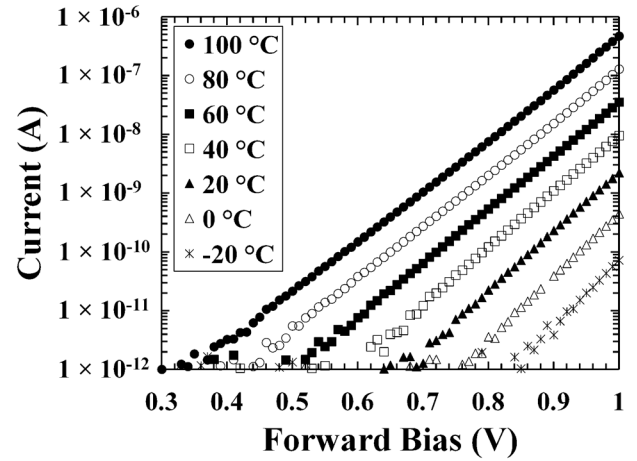


Figure 2. Dark current as a function of applied forward bias for the $\text{In}_{0.5}\text{Ga}_{0.5}\text{P}$ structure at 100 °C (filled circles), 80 °C (empty circles), 60 °C (filled squares), 40 °C (empty squares), 20 °C (filled triangles), 0 °C (empty triangles), and $-20 \text{ }^\circ\text{C}$ (stars).

applied forward bias; the voltage range studied was from 0 V to 1 V (in 0.01 V increments). The uncertainty associated with a single current reading was 0.3% of its value plus 400 fA, while the uncertainty associated with the applied biases was 0.1% of their values plus 1 mV [28]. Preliminary dark current measurements as a function of forward bias were performed on the $\text{In}_{0.5}\text{Ga}_{0.5}\text{P}$ device over the temperature range $-20 \text{ }^\circ\text{C}$ to 100 °C, and shown in figure 2. The decreased dark current observed at $-20 \text{ }^\circ\text{C}$, with respect to the one observed at 100 °C, could be attributed to the lower thermal energy available at lower temperatures. Because of the dependence between dark current and applied forward bias in a simple p-n diode ($I = I_0 \exp\{qV/nkT\}$) [29], it was possible to calculate the saturation current and the ideality factor of the $\text{In}_{0.5}\text{Ga}_{0.5}\text{P}$ device at each temperature: the relation between the dark current and the applied forward bias was linearised as $\ln I = A + BV$ and a linear least square fitting was used to find $A = \ln I_0$ and $B = q(nkT)^{-1}$. The logarithm of the measured saturation current and the calculated ideality factor as a function of temperatures are shown in figures 3(a) and (b), respectively. It was found that the saturation current and the ideality factor decreased as a function of temperature; an ideality factor >1.5 was obtained at all the temperatures studied, highlighting that the generation-recombination mechanism was dominant over the diffusion mechanism [29].

Current characteristics as a function of applied forward bias were then measured under the illumination of the ^{63}Ni radioisotope beta particle source in the temperature range $-20 \text{ }^\circ\text{C}$ and 100 °C. Figure 4 shows the illuminated current as a function of forward bias for the $\text{In}_{0.5}\text{Ga}_{0.5}\text{P}$ device at the temperatures studied. It can be observed that the shape of the experimental curves differed at temperature below 40 °C, this may be due to the conductive mechanism not being negligible with respect to the thermal mechanism (scattering) at low temperatures. The conductive contribution may be responsible for changes in the material resistance due to the increase number of carriers generated as the beta electrons deposit their energy along their tracks in the $\text{In}_{0.5}\text{Ga}_{0.5}\text{P}$ structure.

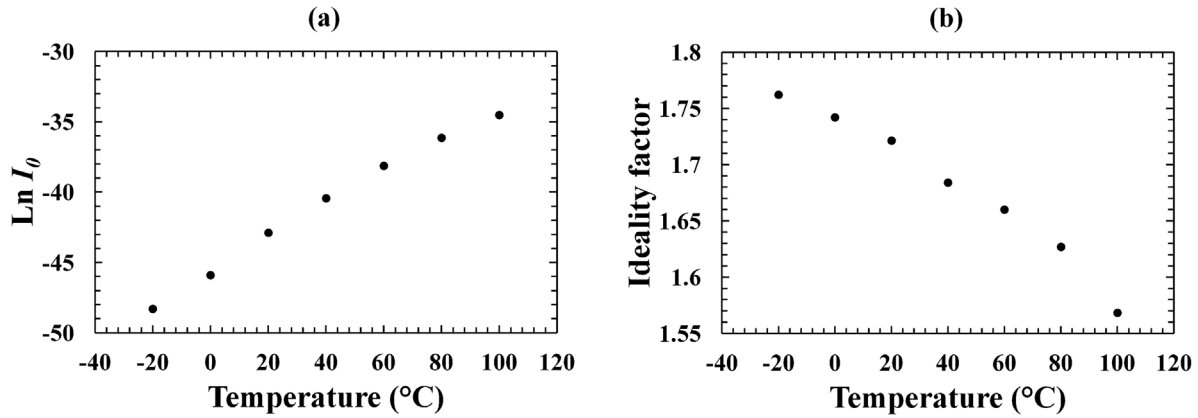


Figure 3. (a) The logarithm of the saturation current as a function of temperature for the $\text{In}_{0.5}\text{Ga}_{0.5}\text{P}$ photodiode. (b) Ideality factor as a function of temperature for the $\text{In}_{0.5}\text{Ga}_{0.5}\text{P}$ device.

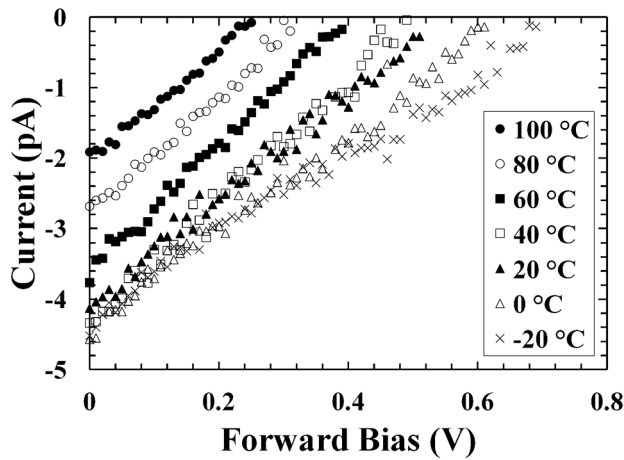


Figure 4. Current as a function of applied forward bias for the $\text{In}_{0.5}\text{Ga}_{0.5}\text{P}$ structure illuminated with the ^{63}Ni radioisotope beta particle source at 100 $^{\circ}\text{C}$ (filled circles), 80 $^{\circ}\text{C}$ (empty circles), 60 $^{\circ}\text{C}$ (filled squares), 40 $^{\circ}\text{C}$ (empty squares), 20 $^{\circ}\text{C}$ (filled triangles), 0 $^{\circ}\text{C}$ (empty triangles), and -20 $^{\circ}\text{C}$ (stars).

The interception points of the illuminated curves on the horizontal and vertical axes corresponded to the open circuit voltage and the short circuit current, respectively. The dependence of such parameters on temperature is shown in figures 5 and 6.

The open circuit voltage (V_{OC}) decreased linearly with increased temperature; in figure 5, the linear least square fit performed on the experimental data is also shown. The variation of the open circuit voltage with temperature was found to be $dV_{OC}/dT = (0.00368 \pm 0.00013) \text{ V } ^{\circ}\text{C}^{-1}$. The $\text{In}_{0.5}\text{Ga}_{0.5}\text{P}$ device illuminated with the ^{63}Ni radioisotope beta particle source had higher V_{OC} values with respect to those previously reported for an $\text{Al}_{0.52}\text{In}_{0.48}\text{P}$ ^{63}Ni radioisotope betavoltaic cell [8]: at -20 $^{\circ}\text{C}$, for example, an open circuit voltage of 0.69 V was observed in the ^{63}Ni - $\text{In}_{0.5}\text{Ga}_{0.5}\text{P}$ cell, whilst 0.52 V was measured in the ^{63}Ni - $\text{Al}_{0.52}\text{In}_{0.48}\text{P}$ cell. This may be explained by the different thicknesses of the $\text{In}_{0.5}\text{Ga}_{0.5}\text{P}$ (5 μm i-layer) and $\text{Al}_{0.52}\text{In}_{0.48}\text{P}$ (2 μm i-layer) devices; the beta-generated carrier density may have been lower in the thicker $\text{In}_{0.5}\text{Ga}_{0.5}\text{P}$ leading to a less significant conductive effect.

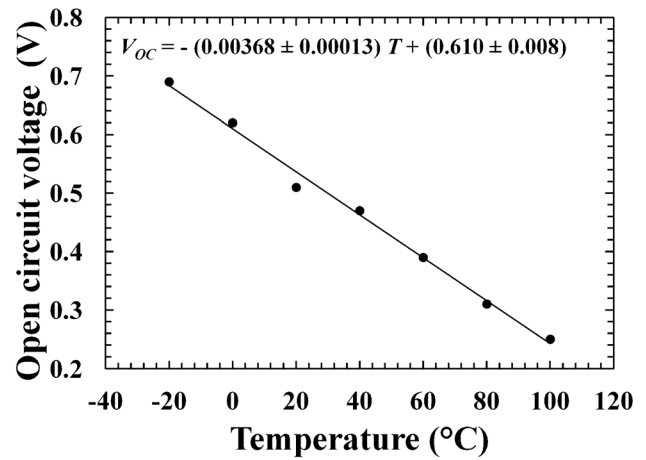


Figure 5. Open circuit voltage as a function of temperature for the ^{63}Ni betavoltaic $\text{In}_{0.5}\text{Ga}_{0.5}\text{P}$ cell; the equation of the line of best fit, as determined by linear least squares fitting is also shown.

The short circuit current (I_{SC}) increased linearly as the temperature was reduced from 100 $^{\circ}\text{C}$ to 40 $^{\circ}\text{C}$, whilst it saturated (~ 4.5 pA) at temperatures below 40 $^{\circ}\text{C}$. A similar behaviour was observed in an $\text{Al}_{0.52}\text{In}_{0.48}\text{P}$ ^{63}Ni radioisotope betavoltaic cell [8]. The short circuit current was found to be dependent on the carrier diffusion length and the number of generated carriers: at increased temperature, while the carrier diffusion length decreased due to the higher phonon scattering, the number of generated carrier increased because of the lower electron-hole pair creation energy. The observed decrease of the short circuit current at higher temperatures from 40 $^{\circ}\text{C}$ to 100 $^{\circ}\text{C}$ may be attributed to a larger decrease in the carrier diffusion length rather than the increase in the number of generated carriers. The approximately constant value assumed by the short circuit current between -20 $^{\circ}\text{C}$ and 40 $^{\circ}\text{C}$ may be explained considering that the conductive mechanism decreased the semiconductor resistance: in such circumstance the decrease in the carrier diffusion lengths (affected by the change in resistance) was possibly compensated by the increase of the number of carriers generated. The conductive mechanism was particularly evident at low temperature and low applied forward bias.

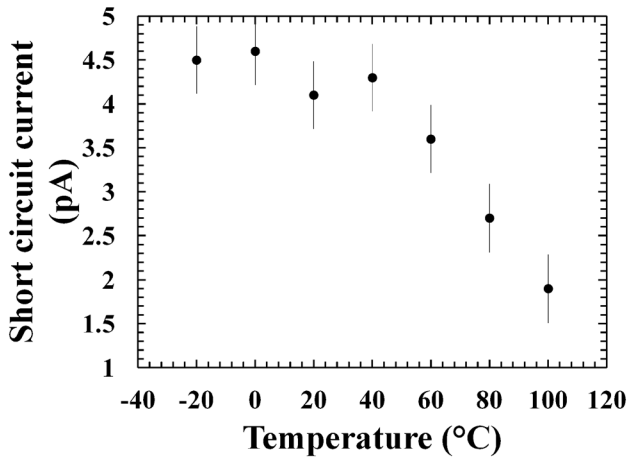


Figure 6. Short circuit current magnitude as a function of temperature for the ^{63}Ni betavoltaic $\text{In}_{0.5}\text{Ga}_{0.5}\text{P}$ cell.

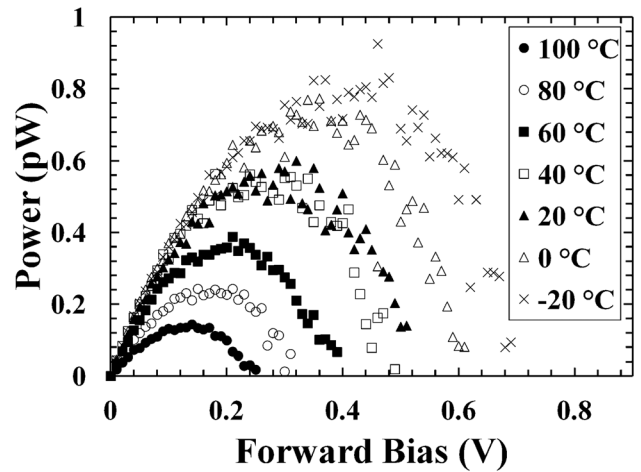


Figure 7. Output power as a function of applied forward bias for the ^{63}Ni betavoltaic $\text{In}_{0.5}\text{Ga}_{0.5}\text{P}$ cell at 100 °C (filled circles), 80 °C (empty circles), 60 °C (filled squares), 40 °C (empty squares), 20 °C (filled triangles), 0 °C (empty triangles), and -20 °C (stars).

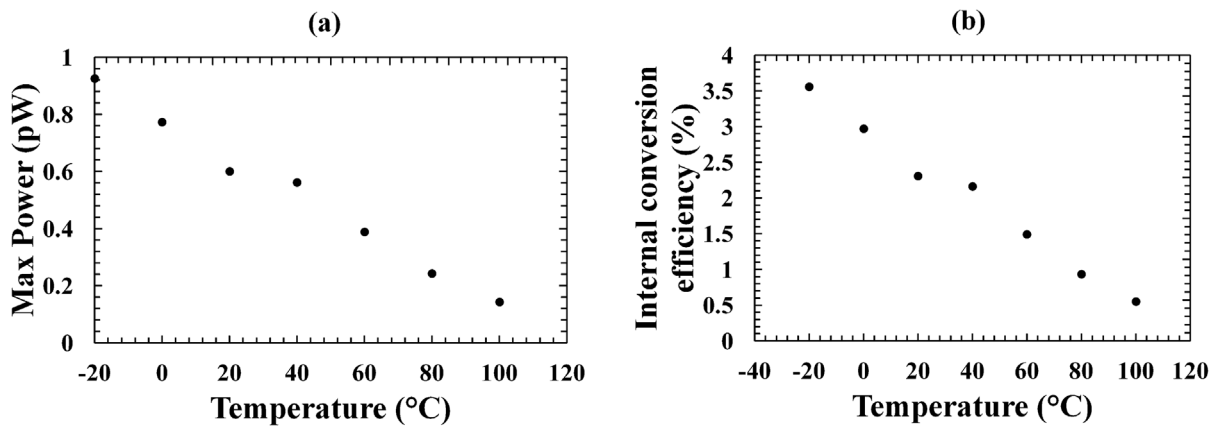


Figure 8. (a) Maximum output power as a function of temperature for the ^{63}Ni betavoltaic $\text{In}_{0.5}\text{Ga}_{0.5}\text{P}$ cell; (b) internal conversion efficiency as a function of temperature for the ^{63}Ni betavoltaic $\text{In}_{0.5}\text{Ga}_{0.5}\text{P}$ cell.

The cell output power (P), calculated as $P = IV$, is shown in figure 7. Increasing the forward bias applied, the output power increased to a maximum (P_m) and then decreased. Figure 8(a) shows the maximum output powers extracted from the $\text{In}_{0.5}\text{Ga}_{0.5}\text{P}$ illuminated with the ^{63}Ni radioisotope beta particle source at temperatures between -20 °C and 100 °C; P_m increased at decreased temperatures, this can be explained considering its dependence on the open circuit voltage [29]. A maximum output power of 0.92 pW, corresponding to 1.2 $\mu\text{W}/\text{Ci}$ (ratio between the maximum output power, 0.92 pW, and the number of electrons expected on the detector taking into account the effects of the inactive Ni overlayer, $2.9 \times 10^5 \text{ s}^{-1} = 7.8 \times 10^{-6} \text{ Ci}$), was extracted at -20 °C. Figure 8(b) shows the internal conversion efficiency (η) values calculated at the different temperatures studied; the internal conversion efficiency was obtained by dividing P_m with P_{th} , the value of which (26 pW) was estimated in section 2. η increased at decreased temperatures, with a value of $\sim 4\%$ being observed at -20 °C.

The maximum output power (P_m) values were higher than the ones observed using an $\text{Al}_{0.52}\text{In}_{0.48}\text{P}$ ^{63}Ni radioisotope

betavoltaic cell [8]: at -20 °C, for example, P_m of 0.92 pW were found here, whilst P_m of 0.28 pW were obtained for the $\text{Al}_{0.52}\text{In}_{0.48}\text{P}$ ^{63}Ni radioisotope betavoltaic cell. The linear dependence of the output power from the open circuit voltage explained the difference in the results reported here from that reported in the $\text{Al}_{0.52}\text{In}_{0.48}\text{P}$ ^{63}Ni radioisotope betavoltaic [8] cells. It should also be noted that the i-layer thickness of the $\text{In}_{0.5}\text{Ga}_{0.5}\text{P}$ structure was 5 μm , whilst the i-layer thickness of the $\text{Al}_{0.52}\text{In}_{0.48}\text{P}$ device was just 2 μm . The InGaP betavoltaic conversion efficiency was higher than those observed for other wide bandgap semiconductors, including GaAs [13] and $\text{Al}_{0.52}\text{In}_{0.48}\text{P}$ [8], particularly at high temperatures. Such conversion efficiency improvement was less evident at lower temperatures, where conductive mechanisms degraded the cell performance.

Improved output power would be expected using a thicker cell and a custom sized ^{63}Ni radioisotope beta source without the inactive Ni over-layer (the ratio between the area of the device, 0.13 mm^2 , and the area of the radioactive ^{63}Ni source, 49 mm^2 , was 0.0026). The use of another $\text{In}_{0.5}\text{Ga}_{0.5}\text{P}$ ^{63}Ni radioisotope betavoltaic cell, placed on top of a ^{63}Ni radioisotope

beta source with two active sides, would also be helpful in order to maximise the conversion of beta energy in electrical energy. Such design improvements will be considered for future generations of radioisotope microbatteries from our laboratory. Next generation of $\text{In}_{0.5}\text{Ga}_{0.5}\text{P}$ ^{63}Ni radioisotope betavoltaic cells will also aim to suppress conductive mechanisms such to exploit the properties (e.g. high linear attenuation coefficient, high bandgap) that make $\text{In}_{0.5}\text{Ga}_{0.5}\text{P}$ attractive as converter layer in betavoltaic microbattery.

4. Conclusions

This paper is the first demonstration of a temperature tolerant $\text{In}_{0.5}\text{Ga}_{0.5}\text{P}$ ^{63}Ni betavoltaic cell. A $\text{p}^+-\text{i}-\text{n}^+$ ($5\ \mu\text{m}$ i-layer) $\text{In}_{0.5}\text{Ga}_{0.5}\text{P}$ mesa diode was illuminated by a $185\ \text{MBq}$ ^{63}Ni radioisotope beta source; the temperature range across which the $\text{In}_{0.5}\text{Ga}_{0.5}\text{P}$ betavoltaic cell was characterised was $-20\ ^\circ\text{C}$ to $100\ ^\circ\text{C}$. The electrical performance of the $\text{In}_{0.5}\text{Ga}_{0.5}\text{P}$ cell was analysed as a function of temperature; the open circuit voltage (V_{OC}), the cell maximum output power (P_{m}), and the cell internal conversion efficiency (η) increased with decreased temperature: V_{OC} of $0.69\ \text{V}$, P_{m} of $0.92\ \text{pW}$, and η of $\sim 4\%$ were found at $-20\ ^\circ\text{C}$. The short circuit current increased as the temperature was decreased from $100\ ^\circ\text{C}$ to $40\ ^\circ\text{C}$, and it saturated to a value of $\sim 4.5\ \text{pA}$ at temperatures $< 40\ ^\circ\text{C}$. This $\text{In}_{0.5}\text{Ga}_{0.5}\text{P}$ ^{63}Ni betavoltaic cell showed better performance than that of an $\text{Al}_{0.52}\text{In}_{0.48}\text{P}$ ^{63}Ni betavoltaic cell [8], most likely as a consequence of the thicker $\text{In}_{0.5}\text{Ga}_{0.5}\text{P}$ structure ($5\ \mu\text{m}$ i-layer) used here compared with the earlier $\text{Al}_{0.52}\text{In}_{0.48}\text{P}$ devices ($2\ \mu\text{m}$ i-layer).

Acknowledgments

This work was supported by STFC grant ST/M002772/1 and ST/P001815/1 (University of Sussex, AMB, PI). The authors are grateful to R J Airey and S Kumar at the EPSRC National Centre for III–V Technologies for device fabrication. M D C Whitaker acknowledges funding received from University of Sussex in the form of a PhD scholarship. A M Barnett acknowledges funding from the Leverhulme Trust in the form of a 2016 Philip Leverhulme Prize.

Data Statement

Data underlying this work are subject to commercial confidentiality. The authors regret that they cannot grant public requests for further access to any data produced during the study.

References

- [1] Kotzar G, Freas M, Abel P, Fleischman A, Roy S, Zorman C, Moran J M and Melzak J 2002 *Biomaterials* **23** 2737
- [2] Trimberger S M and Moore J J 2014 *Proc. IEEE* **102** 1248
- [3] Bower K E, Barbanel Y A, Shreter Y G and Bohnert G W 2002 *Polymers, Phosphors, and Voltaics for Radioisotope Microbatteries* (Boca Raton, FL: CRC Press)
- [4] Chandrashekhar M, Thomas C I, Li H, Spencer M G and Lal A 2006 *Appl. Phys. Lett.* **88** 0335061
- [5] Eiting C J, Krishnamoorthy V, Rodgers S and George T 2006 *Appl. Phys. Lett.* **88** 064101
- [6] Chen H, Jiang L and Chen X 2011 *J. Phys. D: Appl. Phys.* **44** 215303
- [7] Cheng Z, Chen X, San H, Feng Z and Liu B 2012 *J. Micromech. Microeng.* **22** 074011
- [8] Butera S, Lioliou G, Krysa A B and Barnett A M 2016 *J. Appl. Phys.* **120** 144501
- [9] Bormashov V, Troschiev S, Volkov A, Tarelkin S, Korostylev E, Golovanov A, Kuznetsov M, Teteruk D, Kornilov N and Terentiev S 2015 *Phys. Status Solidi a* **212** 2539
- [10] Liu Y, Hu R, Yang Y, Wang G, Luo S and Liu N 2012 *Appl. Radiat. Isot.* **70** 438
- [11] Wang G, Hu R, Wei H, Zhang H, Yang Y, Xiong X, Liu G and Luo S 2010 *Appl. Radiat. Isot.* **68** 2214
- [12] Chandrashekhar M, Duggirala R, Spencer M G and Lal A 2007 *Appl. Phys. Lett.* **91** 053511
- [13] Wang H, Tang X-B, Liu Y-P, Xu Z-H, Liu M and Chen D 2015 *Nucl. Instrum. Methods Phys. Res. B* **359** 36
- [14] Tang X-B, Hong L, Xu Z-H, Liu Y-P and Chen D 2015 *Appl. Radiat. Isot.* **97** 118
- [15] Cabauy P, Olsen L C and Pan N 2013 *US Patent* 8487507 B1
- [16] Cabauy P, Olsen L C and Pan N 2016 *US Patent* 9466401 B1
- [17] Butera S, Lioliou G, Krysa A B and Barnett A M 2016 *J. Phys. D: Appl. Phys.* **49** 355601
- [18] Cress C D, Landi B J, Raffaelle R P and Wilt D M 2006 *J. Appl. Phys.* **100** 114519
- [19] Nelson R J and Holonyak N Jr 1976 *J. Phys. Chem. Solids* **37** 629
- [20] Kuo C P, Vong S K, Cohen R M and Stringfellow G B 1985 *J. Appl. Phys.* **57** 5428
- [21] Ozaki S, Adachi S, Sato M and Ohtsuka K 1996 *J. Appl. Phys.* **79** 439
- [22] Suzuki T, Gomyo A and Iijima S 1988 *J. Cryst. Growth* **93** 396
- [23] Wei S-H and Zunger A 1990 *Appl. Phys. Lett.* **56** 662
- [24] Minagawa S and Kondow M 1989 *Electron. Lett.* **25** 758
- [25] Alam T R and Pierson M A 2016 *J. Energy* **3** 11
- [26] Hovington P, Drouin D and Gauvin R 1997 *Scanning* **19** 1
- [27] Drouin D, Hovington P and Gauvin R 1997 *Scanning* **19** 20
- [28] Keithley Instruments Inc 2011 *Model 6487 Picoammeter/Voltage Source Reference Manual (6487-901-01 Rev B)* (Cleveland, OH: Keithley Instruments Inc.)
- [29] Sze S M and Ng K K 2007 *Physics of Semiconductor Devices* 3rd edn (Hoboken, NJ: Wiley)